Structures in ^{20}O from the ^{14}C(^{7}Li, p) reaction at 44 MeV

Bohlen, HG; von Oertzen, W; Milin, M; Dorsch, T; Krücken, R; Faestermann, T; Hertenberger, R; Mahgoub, M; Wheldon, Carl; Wheldon, Tzanka; Wirth, HF

Document Version
Early version, also known as pre-print

[Link to publication on Research at Birmingham portal](#)

Regular Article – Experimental Physics

Structures in ^{20}O from the ^{14}C(^{7}Li, p) reaction at 44 MeV

H.G. Bohlen[1], W. von Oertzen[1,a], M. Milin[3,b], T. Dorsch[1,2], R. Krücken[2], T. Faestermann[2], R. Hertenberger[4],
Tz. Kokalova[1,c], M. Mahgoub[2], C. Wheldon[1,c], and H.-F. Wirth[2,4]

[1] Helmholtz-Zentrum Berlin, Hahn-Meitner-Platz 1, D-14109 Berlin, Germany
[2] Department of Physics, Faculty of Science, University of Zagreb, Bijenička 32, HR-10000 Zagreb, Croatia
[3] Technische Universität München, James-Franck-Str. 1, D-85748 Garching, Germany
[4] Sektion Physik der Universität München, Am Coulombwall 1, D-85748 Garching, Germany

Abstract. We have studied the multi-nucleon transfer reaction ^{14}C(^{7}Li, p) at $E_{Lab}(^{7}$Li$) = 44$ MeV populating states of the neutron-rich oxygen isotope ^{20}O. The experiments have been performed at the Munich Tandem accelerator using the high-resolution Q3D magnetic spectrometer, with an overall energy resolution of 45 keV. States were populated up to 20 MeV excitation energy —65 states have been identified in the analysis, among which 42 are new. Rotational bands are proposed in terms of underlying intrinsic reflection-asymmetric cluster and prolate molecular structures (namely ^{14}C $\otimes 2n \otimes \alpha$) as parity doublet bands. A rectangular oblate structure is suggested for some very narrow states at high excitation energies.

1 Introduction

Clustering is a general phenomenon in light nuclei, usually at higher excitation energies in the vicinity of the α-decay thresholds [1], as is well known *e.g.* for the α-cluster structures in ^{12}C and ^{16}O. Deformations due to cluster formation are much larger than expected from the standard shell-model structures. Adding neutrons to such cluster systems gives rise to two kind of structures: i) molecular or covalent configurations in which the added ("valence") neutrons induce binding between the clusters based on molecular orbitals [1–3], similar to the well-known effect in atomic physics; ii) "ionic" configurations in which neutrons are concentrated next to one cluster (the one which has larger biding energy for the neutrons). These two types of configurations have been discussed in details, *e.g.*, for the ^{12}Be case [4,5].

Cluster configurations with two clusters of different size, *e.g.* configurations of ^{20}Ne built from α- and ^{16}O-clusters, give rise to intrinsic reflection-asymmetric shapes. Due to this asymmetry these configurations do not have good parity. Following Horiuchi and Ikeda [6], the latter is restored using a linear combination of the wave function describing the given intrinsic shape ϕ_{direct} and its reflection on a plane perpendicular to the symmetry axis,

$\phi_{reflected}$. In this way two bands with opposite parity appear in the excitation spectrum as a so-called parity inversion doublet. States of the bands are defined by parity projection as

$$\Phi_{\pm} = (\phi_{direct} \pm \phi_{reflected})/N_{\pm},$$

where a normalisation contains the non-orthogonality overlap given by

$$N_{\pm}^2 = 2 \left(1 \pm \langle \phi_{direct} \mid \phi_{reflected} \rangle \right).$$

The even- and odd-parity configurations are related to the "+" and the "−" sign, respectively. Parity doublets emerge as two bands with different excitation energies; the energy splitting between the even- and odd-parity bands carries important information on the intrinsic structure of the states, due to the fact that it depends on the overlap integral between the direct and reflected intrinsic shapes. Rotational bands built on these deformed shapes appear, for spin equal to 0, with members $0^+, 2^+, 4^+, \ldots$, for even parity and for odd parity as $1^-, 3^-, 5^-, \ldots$, respectively. Such structures are well known in atomic molecules [7], as well as in heavy nuclei, where this feature appears with octupole deformations as a unique quantum effect [8]. The energy splitting between two bands, E^+-E^-, is usually denoted as $2 \cdot \delta_E$ (see *e.g.* ref. [9]).

In nuclear physics the first reflection-asymmetric cluster structure, suggested by Horiuchi and Ikeda [6], were the (^{12}C $\otimes \alpha$) and (^{16}O $\otimes \alpha$) configurations forming rotational bands in ^{16}O and ^{20}Ne, respectively [10]. Adding

[a] e-mail: oertzen@helmholtz-berlin.de
[b] e-mail: matko.milin@phy.hr
[c] *Present address:* School of Physics and Astronomy, University of Birmingham, Edgbaston, B15 2TT, UK.
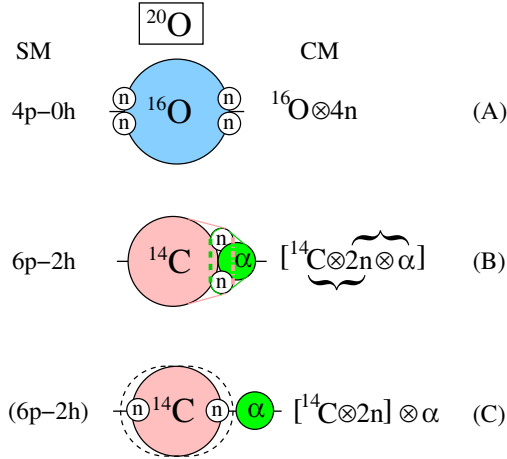
Fig. 1. (Color online) Structures of ^{20}O (schematic, see also ref. [14]), with cluster-model (CM) and shell-model (SM) configurations. (A) the (^{16}O $\otimes 4n$) structure, which characterises the ground-state band and many states of $(sd)^4$-configurations up to 10 MeV; (B) the (^{14}C $\otimes^6$He) structure, where two neutrons are exchanged between the α-particle and the ^{14}C cluster; (C) the "ionic" (^{16}C $\otimes \alpha$) cluster structure (two extra neutrons are concentrated next to the ^{14}C core in ^{16}C). Corresponding SM (p-h) configurations are given.

one or two valence neutrons for example to (^{16}O $\otimes \alpha$) leads to covalent binding in molecular configurations, as *e.g.* in ^{21}Ne and ^{22}Ne. These molecular bonds have been discussed in details by von Oertzen, *e.g.* the (^{16}O $\otimes n \otimes \alpha$) structure for ^{21}Ne [11]. Kimura has performed [12,13] AMD (anti-symmetrised molecular dynamics) calculations for ^{22}Ne, finding the covalent bonds of the two neutrons between the ^{16}O and α-particle. The density plots given in that work for the valence neutrons clearly show the molecular orbital structure with σ- and π-bonds, also well known from the $^{9-10}$Be isotopes [1].

Furthermore, Furutachi *et al.* [14] have calculated cluster and molecular structures for ^{16}O, ^{18}O and ^{20}O in the AMD+GCM framework (GCM —generator coordinate method) and described the parity doublet bands as well as single-particle excitations in these isotopes. The authors deduced for each of the three isotopes the splitting energies between the even- and odd-parity bands of the $K = 0_2^{\pm}$ parity doublets as 3.1 MeV, 4.6 MeV and 6.0 MeV, respectively.

We have performed experimental studies of such structures in ^{18}O, ^{19}O and ^{20}O. The results on ^{18}O [9] and ^{19}O [15] have been published recently —we refer to these articles for a more detailed introduction into the subjects discussed here.

2 Structures in ^{20}O

In the present work rotational bands with parity doublet structures are proposed for ^{20}O in analogy to the ^{22}Ne case (with a ^{14}C cluster instead of ^{16}O). At least two types of cluster configurations are expected to be of importance: "molecular", depicted schematically in fig. 1(B), and

Table 1. Particle thresholds of ^{20}O in units of MeV.

^{19}O + n	^{18}O + 2n	^{16}C + α	^{14}C + ^{6}He	^{14}C + α + 2n
7.608	11.565	12.322	16.817	17.790
^{19}N + p	^{17}O + 3n	^{18}N + d	^{16}O + 4n	^{12}C + 4n + α
19.353	19.608	22.456	23.773	30.915

"ionic" (^{14}C $\otimes 2n$) $\otimes \alpha$ or (^{16}C $\otimes \alpha$), as in fig. 1(C). In the shell-model (SM) framework cluster structures and deformations appear as collective (multi-*particle*–multi-*hole*) excitations (xp-yh). Such structures are well known in the lighter oxygen isotopes, *e.g.* the ($4p$-$4h$) structure of the $K = 0_2^+$ rotational band of ^{16}O at $E_x = 6.05$ MeV (see *e.g.* [16]).

Levels of ^{20}O have been studied previously in a number of reactions [17–25]. The ^{18}O(t, p) reaction was used by Hinds *et al.* at 6 MeV [18], by Pilt *et al.* [20] and LaFrance *et al.* [21,22] at 15 MeV incident energy. States of ^{20}O up to 10.12 MeV excitation energy were found and spins assigned from the analysis of angular distributions. These authors also performed the SM calculations and identified, besides the three states of the ground-state band, three members of the $K = 0_2^+$ band with the band-head at $E_x = 4.458$ MeV. In the SM calculations they have found a pronounced ($6p$-$2h$) structure for these states. This collective, deformed band corresponds to the cluster structure obtained in the AMD calculations of Furutachi *et al.* [14] for the 0_2^+ band-head showing a $[^{14}$C $\otimes^6$He$]$ configuration (see fig. 1(B), adapted from fig. 8(c) of ref. [14]).

Furthermore, two higher-lying 0^+ states have been identified from the following (p, t) data:

i) the state at 5.38 MeV was assigned by Pilt *et al.* [20] definitely as $J^{\pi} = 0_3^+$; it has a shell-model structure. Also LaFrance *et al.* [21] and other authors found in the SM calculations a 70% occupation of the $\nu(1d5/2)^2(2s1/2)^2$ configuration.

ii) The state at 9.770 MeV was assigned with $J^{\pi} = 0_4^+$ by LaFrance *et al.* [21] from the shape of the angular distribution. This 0_4^+ state is located not far from the ^{16}C + α threshold of ^{20}O (table 1), which favours the formation of corresponding cluster structures. The AMD calculations of Furutachi *et al.* [14] show, that at these higher excitation energies cluster structures of the configuration $[^{16}$C $\otimes \alpha]$ are strongly developed (see fig. 1(C), adapted from fig. 8(d) of ref. [14]), note that the 0_4^+ state is labelled in ref. [14] as 0_3^+(AMD) (we added an extra label for the AMD calculation), because the true 0_3^+ state of the experimental level scheme has not been identified in the AMD cluster calculations, probably due in part to its shell-model character).

The odd-parity states in nuclei with the sd-shell are of special interest, because the shell model generally has difficulties to describe them unless a very large basis (with the fp-shells) is used. They appear, however, naturally in connection with the parity doublet structures, rotational

bands based on an asymmetric cluster configuration with axial symmetry. The odd-parity doublet partner to the 0_2^+ band should start with a 1^- state as band-head. Tryggestad *et al.* [23] established two 1^- states at 5.35(10) MeV and 6.85(5) MeV using Coulomb excitation of ^{20}O projectiles at 100 MeV/nucleon. They assigned the state at 5.00(10) MeV as 3^-, which has been already previously observed [20,21], but not finally assigned (3^-, 2^+, 1^-). Wiedekind *et al.* [24] used the complex ^{10}Be(^{14}C, α) reaction with α-γ coincidences and identified again a 1^- state at 5.354 MeV, and in addition, five new states at 3.895 MeV, 4.353 MeV, 4.998 MeV, 5.115 MeV, 5.873 MeV by their γ-transitions, but spin assignments have not been made. Further 3^- and 5^- states have been identified: the 3^- states at $E_x = 5.61$ MeV [21,24], 7.62 MeV [21] and 8.80 [21,19]; these appear all as strong lines in (p, t) reactions. The 5^- states were found at $E_x = 7.252$ MeV and 7.855 [21], these lines are rather weak in (p, t). Sumithrarachchi *et al.* [25] investigated levels of ^{20}O using the β-decay of ^{20}N to final states of ^{20}O. Eight new states were found between 7.570(1) MeV and 12.957(4) MeV from β-γ and β-n coincidences (see tables 4 and 5). They were all assigned with odd parity, but the spin assignments were given only as $(1, 2, 3)^-$, *i.e.* as 1-particle–1-hole excitations typical for β-decay. None of these new states from ref. [24, 25] have been observed in other reactions, and were also not observed in our (^{7}Li, p) reaction, within the given error bars of excitation energies. This observation also points to the fact that our reaction populates dominantly high-spin states with cluster structure. Some states seen in ref. [25] might correspond to the states observed in the present experiment at slightly lower excitation energies, see tables 4 and 5.

3 Experiment

The measurements have been performed at the Tandem Van de Graaff accelerator of the Maier-Leibniz Laboratory of the Technische Universität München and the Ludwig-Maximilians Universität München using the high-resolution Q3D magnetic spectrometer. The ^{14}C(^{7}Li, p)^{20}O reaction has been measured at a beam energy of 44 MeV; the ground-state Q-value for this reaction is +6.842 MeV. States in ^{20}O from the ground state up to excitation energies of 20 MeV have been observed with a resolution of 45 keV using ten different magnetic-field settings. These measurements have been performed at the three scattering angles of $\theta_{Lab} = 10°$, $20°$ and $39°$ with a solid angle of 13.85 msr. Details of the experimental setup and the detector system in the focal plane are given in refs. [9,26]. The ^{14}C target with a total thickness of 70 μg/cm^2 consisted of 89.3% of ^{14}C, 8.6% of ^{12}C and 2.1% of ^{16}O. To determine the corresponding contributions from ^{12}C and ^{16}O in the spectra, measurements on a ^{12}C target of 70 μg/cm^2 thickness and on a V$_2$O$_5$ target of 69 μg/cm^2 thickness with a ^{12}C backing of 20 μg/cm^2 were performed in addition. The corresponding spectra were included in the fit of the ^{20}O spectrum as background contributions and they were normalised to observed characteristic lines of ^{18}O and ^{22}Ne.

The large difference in the masses of projectile and ejectile and the corresponding difference in angular momenta induce a strong mismatch (about 10 $\hbar$) in the angular momentum between incoming and outgoing channels. From this fact it is expected that a direct transfer mechanism is hindered, and a multi-step transfer of the two neutrons and the α-particle favoured; however, the reaction may also proceed partially through a compound-nucleus mechanism. In the latter case the states of higher spin J receive larger cross-sections due to the phase-space factor $(2J + 1)$. This spin multiplicity also applies to direct reactions, a feature which is independent of the structure of states, whether they have cluster or SM structure. A mixture of both reaction mechanisms has already been found in the ^{13}C(^{6}Li, p)^{18}O reaction [27] at the lower incident energy of 28 MeV.

In the analysis of the spectra the lines have been fitted using Gaussian and (above particle thresholds) Breit-Wigner line shapes, and their intrinsic widths have been obtained using the fitting code SPEC [28]. The three-body phase-space distributions for $p + n + {}^{19}$O($E_x = 2.37$ MeV, $J^\pi = 9/2^+$) and $p + p + {}^{19}$N$_{g.s.}$ and the $p + {}^{18}$O$_{g.s.} + 2n$ four-body distribution were also included in the fitting procedure and first normalised in parts of the spectra not having states; the final normalisation is then achieved by simultaneous (least-mean-square) fit of the states and phase-space distributions; details of the procedure can be found in refs. [29,30]. Based on the sensitivity of the fitting procedure, an error in finding the intrinsic widths of the narrowest states is estimated to be $\approx 20\%$, for isolated states it is smaller ($\approx 10\%$).

Spectra with the results of the fitting procedures are shown in fig. 2 for $\theta_{Lab} = 10°$ (upper panel) and $\theta_{Lab} = 39°$ (lower panel). The peaks corresponding to contaminations in the target are marked by the residual nuclei ^{18}O and ^{22}Ne, respectively. The contributions from ^{16}O are extremely small. The contamination spectrum from ^{12}C shows at higher excitation energies itself a smooth rising background (short-dashed line, marked at about $E_x = 20$ MeV by ^{12}C).

In the fit of the spectra Breit-Wigner line shapes were used for unbound states and three- and four-body phase-space distributions were calculated as a background starting at excitation energies at the relevant thresholds —these contribute considerably to the part of the spectrum above the thresholds (see table 1) and can be the origin of some uncertainties in the absolute cross-sections. We observed 65 states (summarised in tables 4 and 5), where only 23 states were known previously from refs. [17–25].

Experimentally observed states at low excitation energies in ^{20}O are generally described rather well within the shell-model calculations (*e.g.* [21]), while for higher excitation energies we found no shell-model calculation published in available literature. The calculation performed within the AMD+GCM framework [14] agrees well with our results regarding moments of inertia of observed configurations, but common shifts in excitation energies are needed to obtain a complete agreement (for details see fig. 3 and sect. 4).
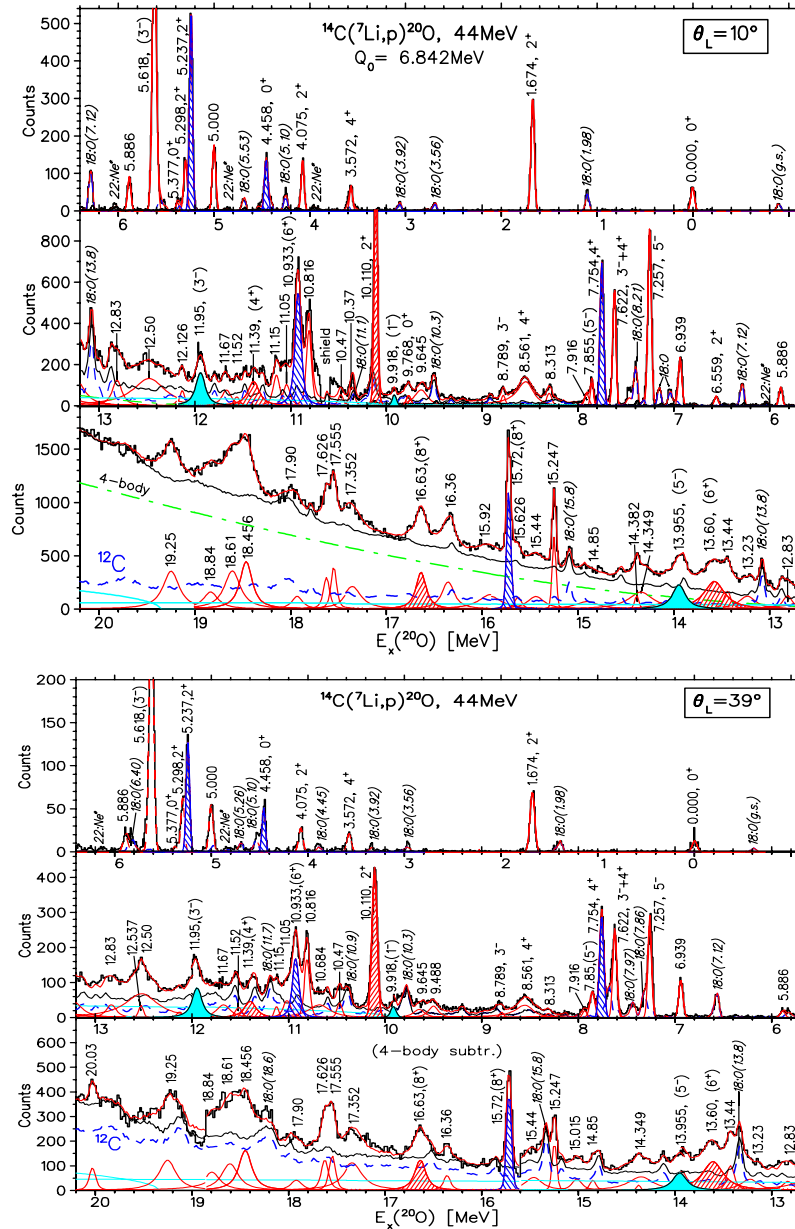
Fig. 2. (Color online) Spectra of the ^{14}C(^{7}Li, p)^{20}O reaction at $E_{Lab} = 44.0$ MeV at $\theta_{Lab} = 10°$ (upper panel) and $\theta_{Lab} = 39°$ (lower panel). The range of excitation energies up to 20.2 MeV is displayed in each panel in three sections. In the upper panel the smooth rising curve (dash-dotted line) represents the $p + {}^{18}$O$_{g.s.} + 2n$ four-body phase-space distribution. This background has been subtracted in the lower panel ($\theta_{Lab} = 39°$). The three-body distributions for $p + n + {}^{19}$O($E_x = 2.37$ MeV, $J^\pi = 9/2^+$) and $p + p + {}^{19}$N$_{g.s.}$ start at 9.98 MeV and 19.35 MeV (continuous lines in both cases), respectively. Spectra measured on ^{12}C and ^{16}O at the same conditions as on ^{14}C are included in the fit, corresponding ^{18}O and ^{22}Ne states are indicated by $18{:}O(E_x)$ and $22{:}Ne(E_x)$, respectively. Members of the $K = 0_2^+$, 0_2^-, and 0_4^+ bands of ^{20}O (with tentative assignments) are marked by downward hatched (blue), filled (cyan), and upward hatched (red) areas, respectively.

4 Discussion of rotational bands

4.1 K $= 0_2^+$ band

LaFrance *et al.* [21] identified the first three members of a cluster band, with the $K = 0_2^+$ band-head at 4.455 MeV (fig. 3, filled blue circles). The straight line corresponds to a linear fit using the relation between the excitation energies $E_x(J)$ and the spins J of a rotational band:

$$E_x(J) = E_{x,0} + J(J+1)\hbar^2/(2\Theta). \qquad (1)$$

The slope of this line is given by $\hbar^2/(2\Theta)$, and depends on the moment of inertia Θ. We attempted to identify higher-lying members of the $K = 0_2^+$ band using: i) the systematics of excitation energies in dependence on $J(J+1)$ by extrapolating the trend to $J = 6$ and $J = 8$, ii) results

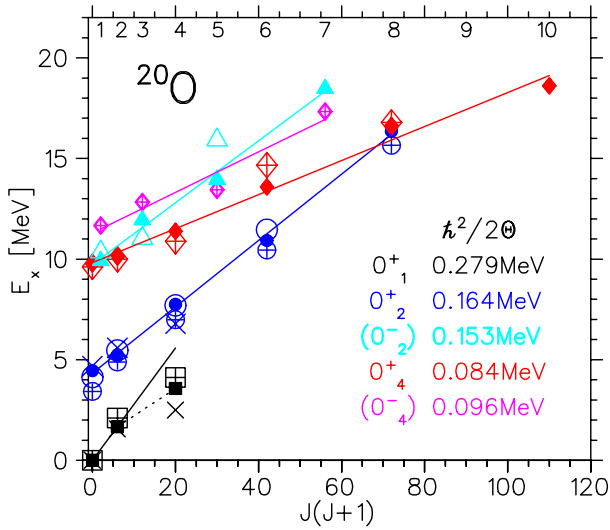**Fig. 3.** (Color online) Rotational band structures proposed for ^{20}O: excitation energies plotted *versus* $J(J+1)$, where J is the spin in units of $\hbar$. The following symbols are used. Ground-state band: filled squares; $K = 0_2^\pm$ parity doublet bands (^{14}C $\otimes$ ^{6}He): filled circles for the 0_2^+ band and filled triangles for the 0_2^- band; $K = 0_4^+$ band: filled diamonds; $K = 0_4^-$ band: open diamonds (magenta); AMD calculations [14] for the $0_2^\pm$ bands: open circles and triangles (shifted by -6.3 MeV); SM calculations using the code Oxbash [31]: open crossed-squares, crossed-circles and crossed-diamonds; GCM (generator-coordinate-method) calculations [32]: ×-crosses. Slope parameters $\hbar^2/2\Theta$ obtained in a linear fit to the data of the rotational bands are given.

from AMD calculations by Furutachi *et al.* [14] (fig. 3, open blue circles) as additional guidance for the relative excitation energies, and iii) the dependence of experimental cross-sections for the band members on $(2J+1)$ at the three angles (fig. 4).

We must add some caution concerning the cross-sections given in tables 4 and 5. Although the same peak positions could be ascertained at the three angles, the overlapping states with a width of 100 keV and more can give strong variations in the yields (factors 1.5–2). Therefore the application of the $(2J+1)$ rule becomes uncertain for states with larger width and the proposed assignments of spin must also be based on other considerations (*e.g.*, on energy systematics) and checked independently.

The data measured at the three angles as well as theoretical two-step transfer calculations do not show characteristic structures of the angular distributions in dependence on J, which would allow spin assignments. Only a faster decrease of the cross-sections towards larger angles is observed for lower spins (see tables 4 and 5). Therefore we do not show the results of these calculations here. Independent of the reaction mechanism, which may be a multi-step transfer of the $(2n+\alpha)$ particles or a statistical compound-nucleus formation (^{21}F*), the cross-sections of the chosen states will be roughly proportional to $(2J+1)$.

This is shown to be approximately fulfilled in the upper part of fig. 4 for the $K = 0_2^+$ band, supporting thus
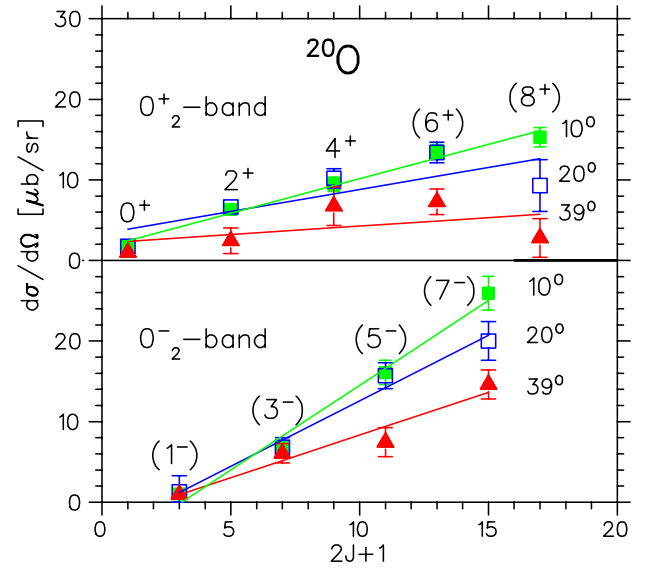
Fig. 4. (Color online) Differential cross-sections in the cm-system for members of the $K = 0_2^+$ (upper panel) and $K = 0_2^-$ (lower panel) rotational bands of ^{20}O, plotted as a function of $(2J+1)$ for three reaction angles. Symbols: filled squares (green), open squares (blue) and filled triangles (red) are used for the cross-sections measured at $\theta_{Lab} = 10°$, $20°$ and $39°$, respectively.

the suggested assignments for the band members. Originally we had chosen for the last entry for the potential 8^+ state the 15.72 MeV state. However, although it seems to fit the energy and cross-section systematics, its width is extremely small indicating a completely different structure. The states placed in the rotational bands are chosen to have larger width for higher spins and excitation energies (the widths are further discussed in the sect. 4.5). For the last member of the band, the potential 8^+ state, the cross-sections start to depart from the $(2J+1)$-rule —this is probably due to a large Q-value mismatch for the states at very high excitation energies. The result for the bands is summarised in table 2. The extremely narrow states are discussed later in sect. 4.6.

4.2 $K = 0_2^-$ band

The band-head of the $K = 0_2^-$ band might be one of the two known 1^- states of ^{20}O at 5.35 MeV and 6.85 MeV [23, 24], but these are not populated in the ^{14}C(^{7}Li, p) reaction and therefore these probably do not have a cluster structure. Also none of the odd-parity states observed by Sumithrarachchi *et al.* [25] in the β-delayed neutron decay of ^{20}N can be identified in our spectra.

The splitting between even- and odd-parity bands of the parity doublet in ^{18}O is estimated to be ≈ 4.0 MeV, based on our results obtained for the ^{12}C(^{7}Li, p) reaction at the same incident energy. Furutachi *et al.* [14] in their AMD calculation predict a splitting energy for the $K = 0_2^\pm$ doublet to be 4.6 MeV for ^{18}O and 6.0 MeV for ^{20}O —the difference between the two is around 1.4 MeV (due to the

Table 2. Experimental excitation energies E_x, spin-parities J^π and widths, given for different K^π rotational bands proposed for ^{20}O: the parity doublet bands 0_2^+ and 0_2^-, and the parity doublet bands 0_4^+ and 0_4^-. Assignments, which are made from the $(2J+1)$, may have to be confirmed independently, and are given in brackets.

$K^\pi = 0_2^+$			$K^\pi = 0_2^-$			$K^\pi = 0_4^+$			$K^\pi = 0_4^-$		
E_x (MeV)	J^π	Γ (keV)	E_x (MeV)	J^π	Γ (keV)	E_x (MeV)	J^π	Γ (keV)	E_x (MeV)	J^π	Γ (keV)
4.458	0^+		9.918	(1^-)	20	9.768	0^+	20	11.67	(1^-)	100
5.237	2^+		11.95	(3^-)	90	10.11	2^+	5	12.83	(3^-)	100
7.754	4^+		13.96	(5^-)	150	11.39	(4^+)	110	13.44	(5^-)	65
10.93	(6^+)	40	18.46	(7^-)	140	13.60	(6^+)	250	17.35	(7^-)	210
16.36	(8^+)	90				16.63	(8^+)	110			
						18.61	(10^+)	190			

fact that one cluster is larger in the ^{20}O case). If we increase the value we obtained for the ^{18}O (4.0 MeV) by this difference, we estimate that the energy splitting for the cluster band in ^{20}O should be around 5.4 MeV. The corresponding 1^- band-head is thus expected in the excitation energy region around 10 MeV. There are only very few states in that region. Including other systematic arguments (size of cross-sections, further members of a band structure) the state at 9.918(5) MeV can be selected and tentatively assigned as the (1^-) band-head in agreement with theoretical predictions.

Further members can be identified using states with: i) the slope for the $J(J+1)$-dependence of the excitation energies as for the $K = 0_2^+$ band; ii) approximately linear dependence of the cross-sections on $(2J+1)$. A ^{20}O level at $E_x = 9.884$ MeV is found in the beta-decay studies of ^{20}N [25]; as it is assigned $J^\pi (1,2,3)^-$ it may correspond to the same state proposed here as the 0_2^- band-head. Candidates for further three members of the odd-parity doublet partner up to $J = (7^-)$ are suggested from the above arguments and are given in table 2 and fig. 3.

4.3 $K = 0_4^+$ band

Properties of the excited states of nuclei whose configurations consist of holes in the $1p$-shell and particles in the $2s1d$-shell can be studied in a weak coupling scheme following the idea of Bansal and French [33] and Zamick [34] (see also ref. [15] for the calculation for ^{19}O). For the $6p$-$2h$ states in ^{20}O, LaFrance *et al.* [22] calculated the excitation energy of 4.4 MeV, which coincides with the excitation energy of the 0_2^+ state. Using the same parameters ($a = 0.41$, $b = 4.9$ and $c = 0.34$, all in MeV) to find the $8p$-$4h$ states (6 particles are neutrons, and 2 are protons), one gets $E_x(8p\text{-}4h) \approx 6.65$ MeV, a surprisingly low value. So further complicated configurations (and their mixing) are expected to occur already at low excitation energies.

So it should not be unexpected that a band with an even higher moment of inertia than the 0_2^+ is proposed to start with the 0_4^+ state at 9.77(1) MeV and the 2^+ state at 10.125(11) MeV. Both states have been identified and have clearly assigned spins and parities from the ^{18}O(p,t) reaction [21]. We observe both states at 9.768(5) MeV and

10.110(4) MeV, respectively, well below the ^{16}C threshold. For the $(^{14}$C $\otimes 2n \otimes \alpha)$ structure the threshold is rather high, however, the pairing effect between the two valence neutrons is known to be large (8 MeV), since a similar effect has been seen in the case of ^{10}Be [1]. This $K = 0_4^+$ band is suggested to have a mixture with an intrinsic $(^{16}$C $\otimes \alpha)$ molecular structure. The covalent structure can be hindered in this case, because the binding energies of the two neutrons are very different in $(^{16}$C$)$ and ^{6}He (no resonant exchange as in ^{21}Ne). Higher-lying band members are tentatively assigned, selecting states which have large cross-sections, proportional to $(2J+1)$, and which follow the $J(J+1)$-dependence on excitation energy. The results are given in table 2 and displayed in fig. 3.

4.4 $K = 0_4^-$ band

In table 3 we list the moments of inertia for different rotational bands found in spectra of oxygen and neon isotopes, as well as the energy splitting of the parity doublets. From

Table 3. Cluster and molecular rotational bands in some oxygen and neon isotopes. The slope parameters $(\hbar^2/2\theta)$ are given for both positive- and negative-parity bands of a given structure. The last column gives the energy splitting $(2 \cdot \delta_E)$ of the parity doublets.

Nuclide	Band-head	$\pi = +$ $\hbar^2/2\theta$ (keV)	$\pi = -$ $\hbar^2/2\theta$ (keV)	Energy splitting (MeV)
^{16}O	0_2^+	231	205	2.9
^{18}O	0_2^+	197	198	4.0
^{18}O	0_4^+	114	115	2.4
^{19}O	$3/2_2^+$	201	195	3.8
^{20}O	0_2^+	164	153	5.2
^{20}O	0_4^+	84	96	1.7
^{20}Ne	0_1^+	167	191	4.8
^{22}Ne	0_2^+	110	105	2.0
^{22}Ne	0_3^+	85	85	1.0

these systematics we can predict that the energy split-ting of the ^{20}O molecular cluster band should be around 2.0 MeV, given that the negative-parity band-head should be expected at around $E_x(0_4^+) + 2\delta_E + 0.1 \cdot J(J+1) = 11.7$ MeV. At $E_x = 11.67$ MeV one can indeed find a state in fig. 2, which then might be assigned 1^- as the band-head of the negative-parity molecular band. Further mem-bers of the band could be the states at $E_x = 12.83$, 13.44 and 17.35 MeV —the corresponding cross-sections show the correct trend to follow the $(2J+1)$ rule. Independent spin/parity assignment are, of course, necessary. See also the discussion in sect. 4.7.

4.5 Widths of the states in the proposed rotational bands

Table 2 lists the states of the proposed doublets of rota-tional bands. There is a general trend for the widths of the states in every rotational band to grow with increas-ing excitation energy, but one can also see non-negligible exceptions. There are several possible reasons for this, one of them certainly being the fact that particle decay of the states in the bands proceeds not only through the ground state of the clusters involved, but also via their excited states. A similar situation is seen in the ^{10}Be case [35–37]: the highest known state of the 0_2^+ molecular band (the one at $E_x = 10.15$ MeV) was actually found to decay not only through the $\alpha + ^6$He(g.s.) channel, but also through the (unbound) 2^+ excited state of ^{6}He at $E_x = 1.8$ MeV. The same effect should be expected in the ^{20}O case and the ^{14}C $+ ^6$He* decay. Since the 1.8 MeV state in ^{6}He has $J^\pi = 2^+$, the decay of the ^{20}O states has contributions of different L-values and the corresponding widths do not show a simple pattern. Experimental determination of de-cay modes for each state is therefore necessary to make final conclusions on the systematics of the proposed rota-tional bands.

4.6 Extremely narrow states: 14.38, 15.24 MeV and 15.72 MeV

There are states at higher excitation energies, which we did not assign to any of the proposed rotational bands and which have very small width (although they are well above the thresholds for one neutron, two-neutron and α-emission). Those states probably have shapes which are not connected to the structures discussed so far. In the spirit of a "complete spectroscopy", which has been achieved for ^{13}C [38] and ^{14}C [39], we also propose further cluster structures, different from the listed ones. Apart from the proposed prolate cluster and molecular states, one should also observe clustered states of the oblate ge-ometry (the coexistence of prolate and oblate shapes was seen, *e.g.*, in ^{14}C [39]). The states are observed with a very small width (below 5 keV) at high excitation ener-gies, at $E_x = 14.38$ MeV, 15.24 MeV and 15.72 MeV, well above the particle decay thresholds. Whereas the first of them (at 14.38 MeV) is rather weak, the latter two have

intensities of potentially higher-spin states $(4^+, 5^+)$. These states are seen at all angles, however, at the smallest an-gle of $10°$ with a width below 5 keV (see table 5). At this angle the width of peaks have only small contributions from the kinematics and from the emittance of the beam. These states do not fit into the systematics of excita-tion energies and width of the proposed rotational bands, therefore we propose that these are examples of shape isomers.

We may consider the tetrahedral shape (quadrupole moment $Q_2 = 0$ and spin $J = 0$) as suggested by Brink *et al.* [40], as a substructure where four valence neutrons are placed on the four connecting lines. One of the excited $J = 0$ states in ^{16}O in the region of $E_x = 10$–15 MeV may have the tetrahedral shape, but a larger rms radius than the ground state. This state will again have $Q_2 = 0$ and $J = 0$, and our state at 14.38 MeV has a $(2J+1)$ intensity corresponding to $J = 0$ relative to the other states. For the other cited states we suggest that they have oblate shapes and belong to a class of states already observed in ^{14}C (3^-), there with a triangular intrinsic structure, where the neutrons are shared by the three α-particles [39]. The corresponding state with optimum energy for ^{20}O would be the rectangular arrangement of four α-particles, with four neutrons in between the four gaps. The excitation en-ergy is expected to be close to the corresponding threshold (connected to the alpha-condensate proposed at 15.1 MeV in ^{16}O, $J = 0_6^+$). This sharing of the valence particles has been shown for ^{14}C to produce a very strong binding en-ergy. In our case the states are below the $(^{14}$C $+ 2n + \alpha)$ threshold of 17.79 MeV, and below the $(^{16}$O $+ 4n)$ thresh-old (23.7 MeV). Their first spin values are expected to be 4^+ and 5^+, consistent with $(2J+1)$ for the yields observed.

Actually inspecting the full list of states in our study of structures in ^{19}O given in ref. [15], we find in a sim-ilar region of excitation energies at least three states (surrounded by states with a large width) with a fitted width below 10 keV. We suggest that these states are again shape isomers in the spirit discussed here. We can expect that particularly stable isomeric states will ap-pear in the isotopes ^{22}O for tetrahedral and in ^{24}O for rectangular shapes, with quite unusual properties. The closest packing and largest binding energy must be ex-pected for 8 valence neutrons in π-bonds in the oblate ^{24}O configuration.

4.7 Discussion of moments of inertia, parity splitting and binding energies

The parity splitting of the $K = 0_2^+$ band in ^{20}O turns out to be 5.2 MeV, a value slightly larger than for ^{18}O. For the negative-parity states we have selected mainly broad states, as in the case of ^{18}O. The experimental values of the moments of inertia θ (summarised in table 3 and fig. 5) can be interpreted in a semi-classical picture using clus-ter density distributions with Gaussian form factors and known rms radii from refs. [41,42] by varying the distance
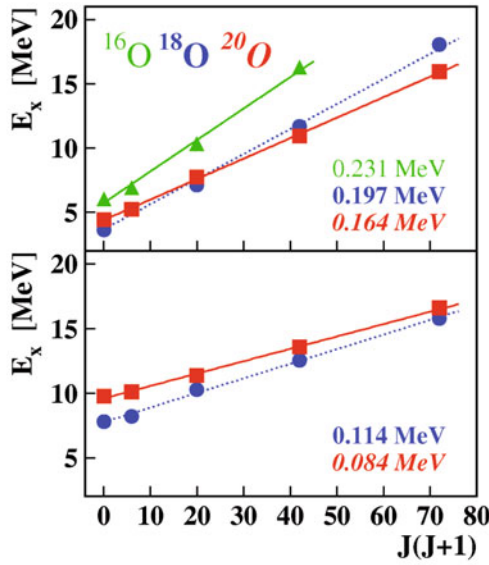
Fig. 5. (Color online) Cluster bands with $\beta_2 \approx 0.4$ and at lower excitation energies (upper part), and higher-lying rotational bands having $\beta_2 \approx 0.6$ with neutrons in valence orbits (lower part) for even oxygen isotopes: ^{16}O (green, triangles, roman values), ^{18}O (blue, circles, bold values) and ^{20}O (red, squares, italic values). The values given in the figure correspond to the slope parameter $(\hbar^2/2\theta)$ for each band (see also table 3).

d between the clusters to reproduce the slope parameters $\hbar^2/2\Theta$ given in fig. 3.

If we assume the $(^{14}$C $\otimes$ ^{6}He$)$ configuration for the lower-lying band (as in ref. [14]), and take the experimentally determined slope parameter (164 keV, see table 3), the procedure results in $d = 3.50$ fm. The same procedure for the higher proposed rotational band (with the ^{16}C $\otimes$ ^{4}He configuration and $\hbar^2/2\theta = 84$ keV) gives $d = 6.35$ fm. Furutachi *et al.* [14] obtained in their AMD calculations for the $K = 0_2^+$ band a distance of 3.65 fm between the ^{14}C and ^{6}He clusters, while in the density plots they have obtained a deformation parameter of $\beta_{intr} = 0.41$. Furthermore, their density plots show also configurations which we can call "ionic", with $\beta_{intr} = 0.61$. These correspond to a pronounced $(^{16}$C $\otimes$ ^{4}He$)$ structure, in particular for the negative-parity states. Actually these configurations are expected to be linked to the σ-configurations for the two neutrons (similar to the case of ^{22}Ne shown in fig. 4 in the work of Kimura [12]). The π-orbitals appear with the band with $\beta = 0.50$ shown in fig. 8e in ref. [14]. The parity splitting for this extended configuration is expected to be quite small. Unfortunately the parity projection of these ^{22}Ne bands has not been done directly —however, we can extract the parity splitting from the fig. 8 of ref. [12] to be around 1.1 MeV, a value close to our experimental result.

The value for the parity splitting of the $K = 0_4^{\pm}$ bands in our work is 1.7 MeV. This value is even smaller than the corresponding value for the ^{18}O molecular band built on 0_4^+ (2.4 MeV, see table 3) indicating that the transition between *direct* and *reflected* configurations is less proba-

ble for the case of ^{20}O —this is probably due to the larger distance between the two major clusters ^{14}C and α. Note that the trend is different for simple cluster configurations ("ionic") —the energy splitting for such bands increases with the number of nucleons, as is the case in the classic example of ^{16}O and ^{20}Ne [6]. This is a consequence of the decreasing distance between the two centres. In molecular configurations with increasing mass number and increasing number of valence neutrons, larger prolate deformations, combined with the higher neutron densities along the symmetry axis, are expected and therefore a smaller energy splitting should be expected. This is the case for the $K = 0_4^{\pm}$ bands in ^{20}O and ^{18}O. A similar effect has been seen for the prolate rotational bands in ^{13}C and ^{14}C [38,39].

From table 3 and fig. 5 it is evident that in both ^{18}O and ^{20}O the bands at higher excitation energies have also higher moments of inertia (*i.e.* lower slope parameters) and smaller energy splittings. For lighter well-studied systems, ^{10}Be [43] and ^{12}Be [4,5], it was found that their higher-lying bands have more "ionic" character, while the lower-lying bands are of molecular nature (*i.e.* with shared neutrons between two clusters), because the delocalisation of neutrons reduces significantly the excitation energy. Similar claims were made for ^{22}Ne [12] and finally for ^{20}O [14], where the lower-lying band was suggested to have mixed ^{14}C $+$ ^{6}He and ^{12}C$+4n+\alpha$ configurations, while the higher-lying one is suggested to correspond to the ^{16}C $+ \alpha$ "ionic" structure. Detailed study of decay modes (especially for exotic decays like ^{5}He- or ^{6}He-emission) should be done to give clear answers on this issue.

Among the unassigned levels at higher excitation energies in tables 4 and 5, one should also look to the proton-hole shell-model states, as found for lighter oxygen isotopes, ^{18}O [9] and ^{19}O [15], as well as carbon isotopes ^{16}C [44] and ^{17}C [45].

Apart from those and other shell-model states and the proposed cluster (prolate and oblate) and molecular rotational bands, in all oxygen isotopes heavier than ^{16}O one should also look for states coupled to the cluster-gas–like state (Hoyle-analogue), recently suggested to be at $E_x(^{16}$O$) \approx 15.1$ MeV [46–48]. The basic structure of such state could be a linear (chain) or rather spherical (tetrahedral) or even oblate configurations [49]. A search for such states should start with a detailed spectroscopy of ^{17}O (through multiple coincidences giving data for decay modes), where first states having a simple cluster character have recently been clearly identified [50]. Among the candidates for states of either oblate or gas-like character in ^{20}O we can identify a number of rather strongly populated states not assigned in our work, see fig. 2. We may expect to get strong binding effects for a closer packing as discussed in sect. 4.6, and although the thresholds for total decomposition are high, the corresponding states may well be those identified as narrow states in sect. 4.6. Further experimental work, in particular studying decay modes of all states and angular correlations between decay products, is needed to complete the spectroscopy of this interesting nucleus and its neighbours.

Table 4. Excitation energies E_x of ^{20}O up to 12.5 MeV, widths of resonances Γ, cross-sections $d\sigma/d\Omega$ in the centre-of-mass system at $\theta_{Lab} = 10°$, $20°$ and $39°$ obtained from the present measurement of the ^{14}C(^{7}Li, p)^{20}O reaction at $E_{Lab} = 44$ MeV, J^π assignments as discussed in the text, and results from the literature. Entries *cont.* or *shield* in the columns of cross-sections indicate that a contamination line or a shielding plate at this place covered the corresponding line of ^{20}O (see also text).

E_x [MeV] This work	Γ [keV]	$\left(\frac{d\sigma}{d\Omega}\right)_{cm}$ [μb/sr] $\theta_{Lab}=10°$	$\left(\frac{d\sigma}{d\Omega}\right)_{cm}$ [μb/sr] $\theta_{Lab}=20°$	$\left(\frac{d\sigma}{d\Omega}\right)_{cm}$ [μb/sr] $\theta_{Lab}=39°$	J^π	J^π_{Lit}	$E_{x,Lit}$ Reactions [MeV]	β-decay [25] [MeV]	Ref.
0.000		0.95(15)	0.7(1)	0.33(7)	0^+	0_1^+	0.000		[17]
1.674(4)		4.1(3)	3.9(2)	1.8(2)	2^+	2^+	1.67368(2)		[17]
3.572(4)		0.76(11)	1.2(1)	0.50(6)	4^+	4^+	3.570(3)		[17]
							3.895(5)		[24]
4.075(4)		1.6(1)	1.5(1)	0.66(7)		2^+	4.072(3)		[17]
							4.353(5)		[24]
4.458(4)		1.8(2)	1.8(2)	1.0(1)	0^+	0_2^+	4.456(3)		[17]
							4.598(5)		[24]
						4^+	4.844(8)		[17, 21, 24]
5.000(4)		2.3(2)	1.8(2)	1.2(1)		$(3^-,2^+,1^-)$	5.002(6)		[23, 20]
							5.115(5)		[24]
5.237(5)		6.3(3)	6.7(3)	2.4(2)	2^+	2^+	5.234(5)		[17]
5.298(7)		1.3(1)	1.7(2)	1.24(8)		2^+	5.304(6)		[17]
						1^-	5.35(10)		[23, 24]
5.377(5)		0.25(7)	0.3(1)	0.13(5)		0_3^+	5.387(6)		[17]
5.618(5)		12.3(3)	9.7(3)	7.2(2)		(3^-)	5.614(3)		[21, 24]
							5.873(5)		[24]
5.886(5)		1.2(1)	0.9(1)	0.5(1)					
6.559(5)		0.7(1)	0.6(1)	0.04(3)		2^+	6.557(1)		[17, 24, 25]
						1^-	6.85(5)		[23]
6.939(5)		3.1(2)	3.1(2)	2.5(2)					
7.257(5)		11.8(3)	11.8(4)	5.5(2)		5^-	7.252(8)		[17]
						$(1,2,3)^-$		7.570(5)	[25]
							7.608		n-thresh.
7.622(7)		7.1(3)	10.0(3)	5.1(2)		$3^- + 4^+$	7.622(7)		[21]
7.754(4)		9.5(3)	10.2(3)	6.8(3)	4^+	4^+	7.754(5)		[17]
7.855(5)	5(2)	1.6(1)	1.8(2)	2.1(2)		(5^-)	7.855(6)		[21]
7.916(4)	10(2)	1.0(1)	1.0(1)	0.5(1)					
8.313(9)	33(5)	1.6(1)	1.4(1)	0.36(4)					
8.561(5)	220(15)	12.1(3)	14.8(4)	5.6(2)		4^+	8.554(8)		[17]
8.789(9)	7(3)	0.9(1)	1.0(1)	0.37(5)		3^-	8.804(9)		[21, 19]
						$(1,2,3)^-$		8.860(8)	[25]
						(0^+)	8.962(21)		[21]
						$(1,2,3)^-$		9.024(6)	[25]
9.488(5)	100(10)	*cont.*	2.9(2)	2.4(2)					
9.645(5)	130(20)	5.5(2)	4.8(2)	1.9(1)					
9.768(5)	20(3)	1.1(1)	1.8(2)	*cont.*	0^+	0_4^+	9.770(8)		[21]
						$(1,2,3)^-$		9.884(15)	[25]
9.918(5)	20(3)	1.0(1)	1.7(2)	1.0(1)	(1^-)				
10.110(4)	5(3)	16.0(3)	21.7(5)	11.8(3)	2^+	2^+	10.125(11)		[21, 19]
10.37(5)	20(5)	2.0(5)	*cont.*	*cont.*					
10.47(5)	20(5)	1.3(3)	*cont.*	1.0(1)					
						$(1,2,3)^-$		10.587(2)	[25]
10.684(5)	260(30)	*shield*	12.2(4)	6.1(2)					
10.816(4)	25(5)	7.2(3)	11.4(3)	5.5(2)					
						$(1,2,3)^-$		10.84(1)	[25]
10.933(4)	40(8)	13.5(3)	13.4(3)	7.3(2)	(6^+)				
11.05(4)	50(10)	3.0(2)	2.2(2)	2.6(1)					
11.15(3)	45(10)	4.1(2)	3.5(2)	0.8(1)					
11.39(1)	110(20)	6.1(4)	4.5(2)	4.0(2)	(4^+)				
11.52(1)	50(15)	1.0(1)	2.5(2)	1.3(1)					
11.67(1)	100(50)	3.2(2)	5.3(3)	3.7(2)					
11.95(1)	90(10)	6.6(3)	6.8(3)	6.1(2)	(3^-)				
12.126(5)	25(5)	1.3(1)	0.9(1)	0.6(1)					

Table 5. Continuation of table 4 for excitation energies of ^{20}O above 12.5 MeV: excitation energies E_x, widths of resonances Γ, cross-sections $d\sigma/d\Omega$ in the centre-of-mass system at $\theta_{Lab} = 10°$, $20°$ and $39°$ obtained from the present measurement of the ^{14}C(^{7}Li, p)^{20}O reaction at $E_{Lab} = 44$ MeV, J^π assignments as discussed in the text, and results from the literature (see text for the entry *overlap*).

E_x [MeV]	Γ [keV]	$\left(\frac{d\sigma}{d\Omega}\right)_{cm}$ [μb/sr] $\theta_{Lab} = 10°$	$\left(\frac{d\sigma}{d\Omega}\right)_{cm}$ [μb/sr] $\theta_{Lab} = 20°$	$\left(\frac{d\sigma}{d\Omega}\right)_{cm}$ [μb/sr] $\theta_{Lab} = 39°$	J^π	J^π_{Lit}	$E_{x,Lit}$ [MeV]	Ref.
12.50(3)	400(50)	23.5(5)	16.9(5)	16.5(3)				
						$(1,2,3)^-$	12.52(2)	[25]
12.537(9)	15(5)	<0.2	2.2(2)	0.9(1)				
12.83(2)	100(10)	6.6(3)	4.0(3)	2.8(2)				
						$(1,2,3)^-$	12.96(2)	[25]
13.23(2)	200(20)	11.4(5)	8.0(3)	5.9(2)				
13.44(1)	65(15)	6.3(3)	12.2(4)	5.4(2)	(5^-)			
13.60(1)	250(50)	29.3(5)	16.4(4)	16.9(3)	(6^+)			
13.955(8)	150(20)	16.1(4)	15.7(4)	7.5(2)	(5^-)			
14.349(6)	300(30)	21.1(4)	15.0(4)	10.1(2)				
14.382(8)	4(3)	2.2(2)	1.4(2)	0.5(1)				
14.85(5)	40(7)	2.0(5)	2.1(2)	1.7(1)				
15.015(5)	100(10)	*cont.*	5.5(3)	0.3(2)				
15.247(5)	5(3)	10.2(3)	8.2(3)	5.0(2)				
15.44(2)	200(20)	10.6(3)	7.9(3)	5.6(2)				
15.626(5)	60(10)	3.8(2)	*overlap*	*overlap*				
15.72(1)	2(1)	18.9(4)	12.8(5)	10.3(3)				
15.92(1)	270(40)	15.0(3)	2.0(2)	*cont.*				
16.36(1)	90(40)	15.3(3)	9.3(4)	2.8(2)	(8^+)			
16.63(1)	110(20)	16.8(3)	21.7(5)	9.2(2)	(8^+)			
17.352(8)	210(30)	16.9(3)	25.2(5)	11.9(3)	(7^-)			
17.555(9)	40(10)	9.5(3)	5.4(3)	5.7(2)				
17.626(4)	50(10)	8.1(3)	6.0(3)	6.1(2)				
17.90(3)	120(30)	6.2(2)	3.6(3)	3.4(2)				
18.456(9)	140(20)	25.9(5)	17.6(5)	14.6(3)	(7^-)			
18.61(1)	190(20)	26.9(5)	28.9(7)	11.8(3)	(10^+)			
18.84(5)	190(20)	11.2(3)	7.9(4)	6.4(2)				
19.25(1)	195(20)	28.7(5)		14.2(3)				
20.03(1)	50(10)			3.7(2)				

5 Summary

We conclude that with the present multi-particle transfer reaction it was possible to observe a large number of new states in ^{20}O of higher spin and with potential cluster structure at higher excitation energies. The reaction did not populate the states found in β- and γ-decay studies. We have found evidence for rotational bands as parity inversion doublets, the proposed bands are summarised in fig. 3. These are the $K = 0_1^+$ ground-state band (shell model) with an $(sd)^4$ configuration of four neutrons on a closed-shell ^{16}O core, the $K = 0_2^\pm$ parity doublet bands with the proposed "ionic" structure with a prolate shape and deformation parameter $\beta_2 = 0.41$. The prolate $K = 0_4^\pm$ band with a more extended molecular (^{14}C $\otimes 2n \otimes \alpha$) structure (deformation parameter $\beta_2 = 0.61$), which may be mixed with a (^{16}C $\otimes \alpha$) configuration. Very narrow states are observed at high excitation energies (14–16 MeV); it is proposed that these are shape isomers, *i.e.* states corresponding to an oblate structure of rectangular shape.

References

1. W. von Oertzen, M. Freer, Y. Kanada-En'yo, Phys. Rep. **432**, 43 (2006).
2. W. von Oertzen, Z. Phys. A **354**, 37 (1996).
3. W. von Oertzen, Z. Phys. A **357**, 355 (1997).
4. M. Ito, N. Itagaki, H. Sakurai, K. Ikeda, Phys. Rev. Lett. **100**, 182502 (2008).
5. M. Ito, N. Itagaki, Phys. Rev. C **78**, 011602(R) (2008).
6. H. Horiuchi, K. Ikeda, Prog. Theor. Phys. **40**, 277 (1968).
7. G. Herzberg, *Molecular Spectra and Molecular Structure*, Vol. **I**, *Spectra of Diatomic Molecules* (Van Nostrand Reinhold, New York, 1950) p. 129.
8. P.A. Butler, W. Nazarewicz, Rev. Mod. Phys. **68**, 350 (1996).
9. W. von Oertzen *et al.*, Eur. Phys. J. A **43**, 17 (2010).
10. H. Horiuchi, *Clusters in Nuclei*, edited by C. Beck, Vol. **1** (Springer, Berlin, 2010) (Lect. Notes Phys. **818**, 57 (2010)).
11. W. von Oertzen, Eur. Phys. J. A **11**, 403 (2001).
12. M. Kimura, Phys. Rev. C **75**, 034312 (2007).
13. Y. Kanada-En'yo, M. Kimura, *Clusters in Nuclei*, edited by C. Beck, Vol. **1** (Springer, Berlin, 2010) (Lect. Notes Phys. **818**, 129 (2010)).
14. N. Furutachi *et al.*, Prog. Theor. Phys. **119**, 403 (2008).
15. W. von Oertzen *et al.*, Eur. Phys. J. A **46**, 345 (2010).
16. K. Wildermuth, Y.C. Yang, *A Unified Theory of the Nucleus* (Vieweg, Braunschweig, 1977).
17. D.R. Tilley *et al.*, Nucl. Phys. A **636**, 249 (1998).
18. S. Hinds *et al.*, Nucl. Phys. **38**, 81 (1962).
19. R. Jahn *et al.*, Phys. Rev. C **18**, 9 (1978).
20. A.A. Pilt *et al.*, Phys. Rev. C **19**, 20 (1979).
21. S. LaFrance *et al.*, Phys. Rev. C **20**, 1673 (1979).
22. S. LaFrance, H.T. Fortune, S. Mordechai, R. Middleton, J. Phys. G **5**, L59 (1979).
23. E. Tryggestad *et al.*, Phys. Rev. C **67**, 064309 (2003).
24. M. Wiedeking *et al.*, Phys. Rev. Lett. **94**, 132501 (2005).
25. C.S. Sumithrarachchi *et al.*, Phys. Rev. C **74**, 024322 (2006).
26. T. Dorsch, PhD Thesis, TU München and Helmholtz-Zentrum Berlin (2008).
27. M.J. Smithson *et al.*, Phys. Rev. C **37**, 1036 (1988).
28. H.G. Bohlen, *Code SPEC (Version F)*, HMI Berlin, private communication (2003).
29. H.G. Bohlen, H. Ossenbrink, H. Lettau, W. von Oertzen, Z. Phys. A **320**, 237 (1985).
30. E. Adamides, H.G. Bohlen, W. von Oertzen *et al.*, Nucl. Phys. A **475**, 598 (1987).
31. W. Rae, A. Etchegoyen, B.A. Brown, *OXBASH shell model code*, Technical Report no. 524 (MSU Cyclotron Laboratory, 1985).
32. P. Descouvemont, Phys. Lett. B **437**, 7 (1998).
33. R. Bansal, J.B. French, Phys. Lett. **11**, 145 (1964).
34. L. Zamick, Phys. Lett. **19**, 580 (1965).
35. M. Freer *et al.*, Phys. Rev. Lett. **96**, 042501 (2006).
36. Đ. Miljanić *et al.*, Fizika (Zagreb) B **10**, 235 (2001).
37. M. Milin *et al.*, Nucl. Phys. A **753**, 263 (2005).
38. M. Milin, W. von Oertzen, Eur. Phys. J. A **14**, 295 (2002).
39. W. von Oertzen *et al.*, Eur. Phys. J. A **21**, 193 (2004).
40. D. Brink, H. Friedrich, A. Weiguny, C.W. Wong, Phys. Lett. B **33**, 143 (1970).
41. H. de Vries *et al.*, At. Data Nucl. Data Tables **36**, 495 (1987).
42. K. Arai *et al.*, Phys. Rev. C **59**, 1432 (1999).
43. M. Ito, Phys. Lett. B **636**, 293 (2006).
44. H.G. Bohlen *et al.*, Phys. Rev. C **68**, 054606 (2003).
45. H.G. Bohlen *et al.*, Eur. Phys. J. A **31**, 279 (2007).
46. T. Wakasa *et al.*, Phys. Lett. B **653**, 173 (2007).
47. Y. Funaki *et al.*, Phys. Rev. C **80**, 064326 (2010).
48. Y. Funaki, private comunication.
49. W. von Oertzen, *Clusters in Nuclei*, edited by C. Beck, Vol. **1** (Springer, Berlin, 2010) (Lect. Notes Phys. **818**, 109 (2010)).
50. M. Milin *et al.*, Eur. Phys. J. A **41**, 335 (2009).